Neurosci Bull April 1, 2014, 30(2): 217–232. http://www.neurosci.cn
DOI: 10.1007/s12264-013-1421-0

·Review·

Disrupted structural and functional brain connectomes in mild cognitive impairment and Alzheimer's disease

Zhengjia Dai[1,2], Yong He[1,2]

[1]*State Key Laboratory of Cognitive Neuroscience and Learning; IDG/McGovern Institute for Brain Research, Beijing Normal University, Beijing 100875, China*

[2]*Center for Collaboration and Innovation in Brain and Learning Sciences, Beijing Normal University, Beijing 100875, China*

Corresponding author: Yong He. E-mail: yong.he@bnu.edu.cn

Alzheimer's disease (AD) is the most common type of dementia, comprising an estimated 60–80% of all dementia cases. It is clinically characterized by impairments of memory and other cognitive functions. Previous studies have demonstrated that these impairments are associated with abnormal structural and functional connections among brain regions, leading to a disconnection concept of AD. With the advent of a combination of non-invasive neuroimaging (structural magnetic resonance imaging (MRI), diffusion MRI, and functional MRI) and neurophysiological techniques (electroencephalography and magnetoencephalography) with graph theoretical analysis, recent studies have shown that patients with AD and mild cognitive impairment (MCI), the prodromal stage of AD, exhibit disrupted topological organization in large-scale brain networks (i.e., connectomics) and that this disruption is significantly correlated with the decline of cognitive functions. In this review, we summarize the recent progress of brain connectomics in AD and MCI, focusing on the changes in the topological organization of large-scale structural and functional brain networks using graph theoretical approaches. Based on the two different perspectives of information segregation and integration, the literature reviewed here suggests that AD and MCI are associated with disrupted segregation and integration in brain networks. Thus, these connectomics studies open up a new window for understanding the pathophysiological mechanisms of AD and demonstrate the potential to uncover imaging biomarkers for clinical diagnosis and treatment evaluation for this disease.

Keywords: connectome; small-world; graph theory; connectivity; MRI; DTI; fMRI; EEG/MEG

Introduction

As of 2010, there were an estimated 35.6 million people with dementia worldwide, and the number is expected to double every 20 years, with 65.7 million in 2030 and 115.4 million in 2050 (World Alzheimer Report 2010, http://www.alz.org). Alzheimer's disease (AD) is the most common type of dementia, comprising an estimated 60–80% of all dementia cases. Difficulty in remembering names and recent events is usually an early clinical symptom of AD; apathy and depression are early symptoms as well. Later symptoms include impaired judgment, disorientation, confusion, behavioral changes, and difficulties in speaking, swallowing, and walking. AD is ultimately fatal. In 2011, the National Institute on Aging and the Alzheimer's Association proposed new criteria and guidelines for diagnosing AD[1-4]. Accordingly, the three stages are preclinical AD, mild cognitive impairment (MCI) due to AD, and dementia due to AD. In preclinical AD, individuals have measurable changes in the brain but have not yet developed symptoms such as memory loss. Although the new criteria and guidelines identify the preclinical form as a stage of AD, they do not establish immediately useful diagnostic criteria. Further, the guidelines state that additional research on biomarker tests

is needed before this stage of AD can be diagnosed. In MCI, individuals have cognitive impairments beyond what is expected for their age and education, without substantial interference with daily activities, and they have a high risk of progression to AD[5].

Previous studies have demonstrated that the clinical manifestations of AD are not only associated with regional gray matter damage but also with abnormal integration between brain regions through disconnection mechanisms[6-8]. With the advent of non-invasive structural and functional neuroimaging and neurophysiological techniques, it has become possible to assess *in vivo* aberrant cortico-cortical axonal pathways and synchronizations of neuronal activity (i.e., connectomics) in AD patients. Recently, graph theoretical analysis has provided a unique tool to reveal intrinsic attributes of the connectivity patterns of a complex network/graph from the global perspective. Within this framework, a complex brain system can be formalized as a mathematical model consisting of a set of nodes and a set of pairwise relationships between the nodes (i.e., edges). Topological metrics of brain networks such as small-world, modularity, and hubs[9-11] are often used to explore the structural and functional connectivity patterns of the human brain.

In this article, we review the recent progress in AD-related brain network research, focusing specifically on the changes of topological organization in the large-scale structural and functional brain networks, using graph theoretical approaches.

Brain Network Measures

In graph theory, a network is defined as a graph comprising a set of nodes or vertices and the edges or lines between them. In a large-scale brain network, nodes usually represent electroencephalograph (EEG) electrodes, magnetoencephalograph (MEG) channels, and imaging voxels or regions of interest (ROIs) derived from anatomical or functional atlases, while links represent the structural or functional associations among nodes. The structural associations can be defined as covariations of cortical thickness or volume between the ROIs across individuals or diffusion magnetic resonance imaging (dMRI)-traced white matter tracts. The functional associations can be defined as temporal correlations and can be measured with either linear or nonlinear techniques in EEG/MEG and functional MRI (fMRI). The network types can be classified as directed or undirected, based on whether the edges have directional information, and as weighted or binary, based on whether the edges have weighting information. The present review focuses on the undirected binary or weighted brain networks. The flowchart of brain network construction is presented in Figure 1. Below, we briefly introduce several key network metrics, which are also summarized in Table 1. More detailed descriptions of graph theory can be found in previous publications[12-14].

Segregation Measures

Segregation in the brain is the ability for specialized information processing to occur within densely interconnected groups of regions. Measures of segregation are primarily based on the concepts of clustering coefficient and modularity. The clustering coefficient of a node is given by the ratio of the number of connections between the direct neighbors of the node to the total number of possible connections between these neighbors. The clustering coefficient of a network is calculated by averaging the clustering coefficients over all nodes in the network. Thus, the clustering coefficient provides information about the level of local connectedness within a network, a higher value representing higher local efficiency of information transfer. Another important measure of segregation is modular structure, which can be reflected by the single statistic of modularity. Each module contains several densely interconnected nodes, and there are relatively few connections between nodes in different modules[15].

Integration Measures

Integrative processes in the brain can be considered from at least two angles, one based on the efficiency of global information communication and the other on the ability of the network to integrate distributed information. Measurement of the efficiency of global information communication in a network is commonly based on the characteristic path length, which is the average minimum number of connections that link any two nodes of the network. On the other hand, the ability of a network to integrate distributed information can usually be revealed by the network hubs, which are nodes with high levels of degree or other node measures of centrality. The degree of a node is the number of edges that link to this node.

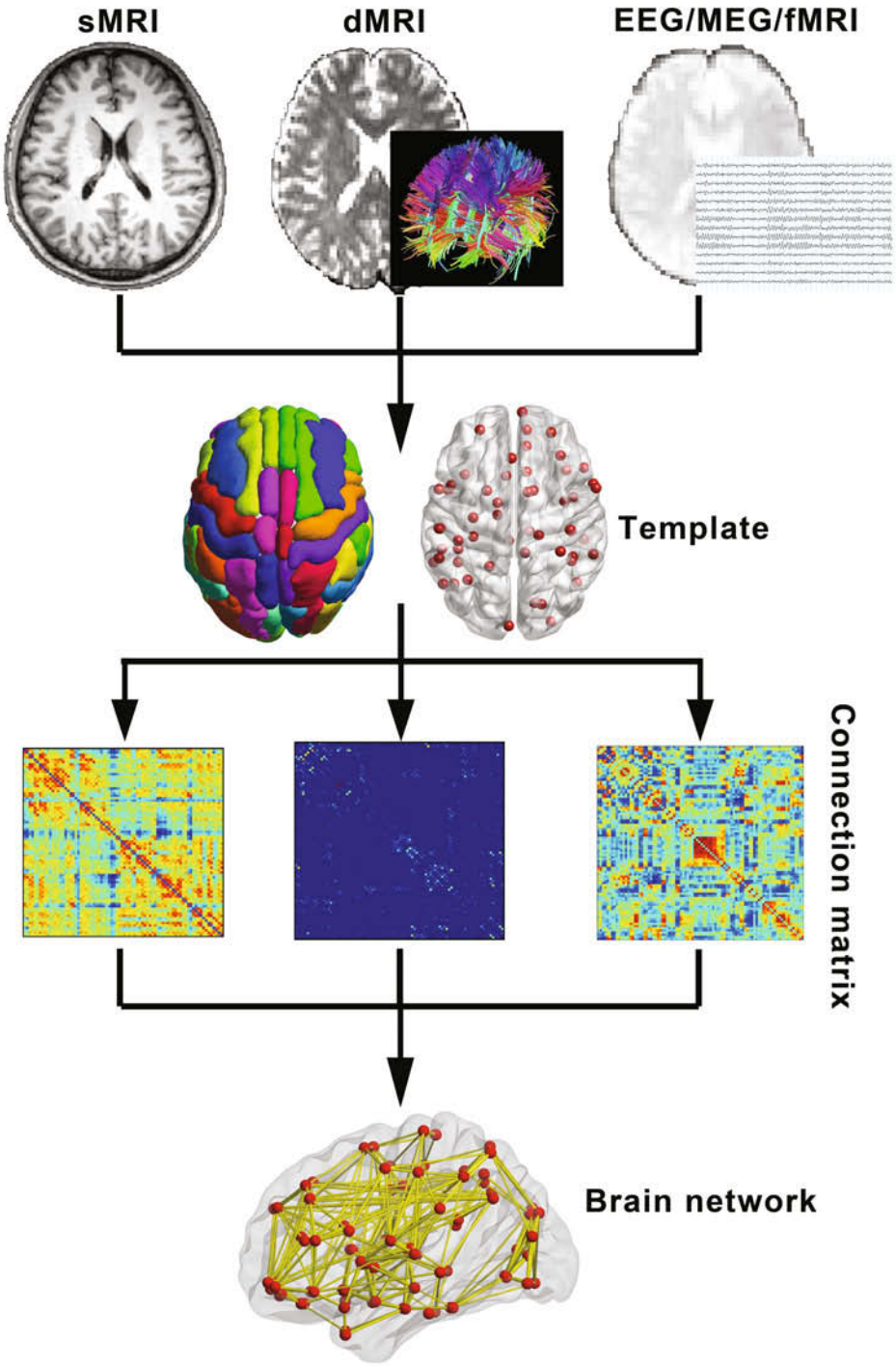

Fig. 1. Flowchart for construction of structural and functional brain networks. First is the extraction of gray-matter morphological metrics such as cortical thickness and gray-matter volume from structural MRI (sMRI) data, and the white-matter fiber information such as fiber number from diffusion MRI (dMRI) or the time-course from EEG/MEG/fMRI. Second, the nodes of the brain network are obtained from prior brain templates (e.g., anatomical templates, random templates, functional templates, or voxel-based schemes). Third, region-based or voxel-based information is extracted from the above imaging data. All pair-wise associations between nodes are calculated to generate a connection matrix. Finally, the connection matrix is visualized.

Table 1. Segregation and integration network measures

Measure	Description
Measures of segregation	
Clustering coefficient	The clustering coefficient quantifies the number of connections that exist between the nearest neighbors of a node as a proportion of the maximum number of possible connections. It measures the extent of local clustering of the network.
Modular structure	Modular structure is defined by a high density of connectivity among nodes of the same module and a low density of connections between nodes of different modules.
Measures of integration	
Characteristic path length	The characteristic path length of a network is the average minimum number of connections that link any two nodes of the network. It measures the overall routing efficiency of the network.
Hubs	Hubs are nodes with high levels of connection edges or other node measures of centrality.

Other measures of centrality mainly include betweenness centrality and eigenvector centrality. The betweenness centrality of a node measures how many of the shortest paths between all other node pairs in the network pass through that node[16], while the eigenvector centrality is simply the eigenvector of the adjacent matrix corresponding to the largest eigenvalue[17].

Small-world Network

Based on the two network information-processing perspectives of information segregation and integration, different types of networks can be distinguished, including regular, small-world, and random networks. A small-world network has a shorter characteristic path length than a regular network (high clustering coefficient and long characteristic path length) and a greater clustering coefficient than a random network (low clustering coefficient and short characteristic path length)[18]. To quantitatively examine the small-world properties, normalized characteristic path length and normalized clustering coefficient are computed. The normalized characteristic path length is defined as the ratio of the characteristic path length of the brain network to that of matched random networks, while normalized clustering coefficient is defined as the ratio of the clustering coefficient of the network to that of matched random networks. Typically, the ratio between the normalized characteristic path length and the normalized clustering coefficient should be >1 for a small-world network. Notably, small-world structure characterizes an optimized balance between segregation and integration, which is essential for high synchronizability and fast information transmission in a complex network. Deviation from this optimal configuration, such as disrupted integration and segregation, may lead to various brain disorders.

Brain Networks in AD and MCI

By searching PubMed (http://www.ncbi.nlm.nih.gov/pubmed) using the keywords “graph theory”, “small-world”, “connectome”, “Alzheimer’s disease”, and “mild cognitive impairment”, we selected articles that used graph theory to analyze networks at the whole-brain level based on MRI and EEG/MEG data (Table 2). Other work included connectomics reviews, mainly focusing on the altered network properties in AD populations but paying little attention to MCI populations[19-21]. In addition, with the widespread application of graph theory in the study of brain networks, the number of AD-related brain network studies is growing rapidly. Here, we include 25 papers, many more than in previous reviews, and this is the first review based on the two perspectives of information segregation and integration.

Structural Connectomics in AD and MCI

The network of structural connectomics in the human brain *in vivo* can be constructed using both structural MRI (sMRI) and dMRI. In this section, we review recent progress in analyzing the structural and diffusion MRI networks in AD and MCI.

Table 2. Overview of large-scale structural and functional brain network studies in MCI and AD

Study	Modality	Group	Subject *n* (Male)	Age*	MMSE*	Network type	Node numbers	Connectivity metrics	Main findings
He *et al.*, 2008[26]	sMRI	AD HC	92 (38) 97 (26)	62-96 60-94	14-30 25-30	B	54	Partial correlation of the regional cortical thickness	(1) Higher clustering coefficient and characteristic path length in the structural brain networks of AD. (2) Decreased topological centrality in temporal and parietal areas and increased centrality in the occipital regions in AD.
Yao *et al.*, 2010[27]	sMRI	AD MCI HC	91 (50) 113 (79) 98 (49)	55.73-90.20 56.28-89.40 70.02-90.74	nr nr nr	B	90	Pearson's correlation of the regional cortical volume	(1) Higher clustering coefficient and characteristic path length in AD. (2) Intermediate network measures values of MCI, between those of HC and AD.
Tijms *et al.*, 2013[28]	sMRI	AD HC	38 (19) 38 (19)	72.06 ± 4.32 71.91 ± 4.32	19.65 ± 5.42 27.67 ± 2.20	B	8683± 545	Intracortical similarity	(1) Lower small world coefficient, normalized clustering coefficient and normalized characteristic path length in AD. (2) Strongest relationship between characteristic path length and cognitive decline in the parahippocampal gyrus, hippocampus, fusiform gyrus and precuneus in AD.
Lo *et al.*, 2010[34]	DTI	AD HC	25 (15) 30 (19)	79.40 ± 5.89 77.07 ± 6.37	20.92 ± 2.36 28.83 ± 0.99	W	78	Diffusion MRI tractography	(1) Higher characteristic path length and lower global efficiency in white matter network in AD. (2) Reduced nodal efficiency of the frontal regions in AD.
Bai *et al.*, 2012[38]	DTI	aMCI RGD HC	38 (25) 35 (14) 30 (16)	71.6 ± 5.3 67.9 ± 4.5 71.3 ± 4.4	27.03 ± 1.57 28.54 ± 2.19 28.43 ± 1.25	W	90	Diffusion MRI tractography	(1) Lower global efficiency and higher characteristic path length in aMCI and RGD compared with HC. (2) Similar deficits of the regional and connectivity characteristics in the white matter networks of the frontal brain regions in RGD and aMCI patients compared with HC. (3) Different nodal efficienies of the posterior cingulate cortex and several prefrontal brain regions between the patient groups.
Shu *et al.*, 2012[36]	DTI	MD aMCI SD aMCI HC	20 (9) 18 (10) 36 (17)	65.4 ± 7.3 64.8 ± 7.2 63.1 ± 5.3	25.6 ± 1.7 26.8 ± 1.3 28.4 ± 1.7	B	90	Diffusion MRI tractography	(1) Disrupted global topological organization of white matter networks in MD aMCI but not in those with SD aMCI, compared with HC. (2) Impaired connectivity of the temporal, frontal, and parietal cortices in MD aMCI.
Daianu *et al.*, 2013[37]	DTI	AD lMCI eMCI HC	15 (9) 11 (7) 57 (34) 28 (14)	75.6 76.3 73.7 73	nr nr nr nr	W	68	Diffusion MRI tractography	(1) Lower network nodal degree, normalized characteristic path length and efficiency in AD. (2) Higher normalized small-worldness in the whole brain and left and right hemispheres and higher normalized clustering coefficient in the whole brain in AD.
Reijmer *et al.*, 2013[35]	DTI	AD HC	50 (22) 15 (9)	78.8 ± 7.1 77.0 ± 1.5	25 ± 3 28 ± 1	W	90	Diffusion MRI tractography	(1) Lower local efficiency in AD. (2) Positive correlation between efficiency values and memory and executive functioning scores in AD.
Stam *et al.*, 2007[42]	EEG	AD HC	15 (4) 13 (6)	54-77 57-78	15-28 27-30	B	21	Synchronization likelihood	(1) Longer characteristic path length in beta band of AD. (2) Negative correlation between MMSE scores and path length in beta band for all subjects.
de Haan *et al.*, 2009[44]	EEG	AD FTLD HC	20 (7) 15 (12) 23 (14)	51-76 43-79 49-78	14-27 13-30 27-30	B	21	Synchronization likelihood	(1) Lower normalized clustering coefficient in the lower alpha and beta bands, lower normalized characteristic path length in lower alpha and gamma bands and lower mean degree in both alpha frequency bands in AD. (2) Positive correlation between MMSE scores and normalized characteristic path length in AD.
Stam *et al.*, 2009[43]	MEG	AD HC	18 (11) 18 (7)	72.1 ± 5.6 69.1 ± 6.8	13-25 27-30	W	149	Phase lag index	(1) Lower clustering coefficient, normalized clustering coefficient and lower normalized characteristic path length and higher characteristic path length in lower alpha band of AD. (2) Positive correlation between MMSE scores and normalized clustering coefficients in the lower alpha band for all subjects.
Buldu *et al.*, 2011[47]	MEG	MCI HC	19 19	nr nr	nr nr	W	148	Synchronization likelihood	(1) Higher connection strength in MCI. (2) Higher normalized clustering coefficient and lower characteristic path length at broadband signal in MCI.
de Haan *et al.*, 2012[45]	MEG	AD HC	18 (12) 18 (7)	67 ± 9 66 ± 9	23 ± 1 29 ± 1	W	149	Synchronization likelihood	(1) Weaker links within and especially between functional modules and correlation with cognitive dysfunction in AD. (2) Strongest intramodular loss in parietal cortex in AD.

(To be continued)

(Continued)

Table 2. Overview of large-scale structural and functional brain network studies in MCI and AD

Study	Modality	Group	Subject *n* (Male)	Age*	MMSE*	Network type	Node numbers	Connectivity metrics	Main findings
de Haan *et al.*, 2012[46]	MEG	AD HC	18 (12) 18 (7)	67 ± 9 66 ± 9	23 ± 1 29 ± 1	W	149	Synchronization likelihood	(1) Impaired network integrity in AD, especially in the higher frequency bands. (2) Lower eigenvector centrality of the left temporal region in the theta band in AD and positive correlation with MMSE scores.
Supekar *et al.*, 2008[51]	fMRI	AD HC	21 (10) 18 (10)	48-83 37-77	12-29 27-30	B	90	Wavelet correlation	(1) Lower normalized clustering coefficient and normalized unchanged characteristic path length in the functional brain networks (0.01-0.05 Hz) of AD. (2) Lower normalized clustering coefficient in the left and right hippocampus in AD.
Sanz-Arigita *et al.*, 2010[52]	fMRI	AD HC	18 (9) 21 (8)	70.7 ± 7.2 70.7 ± 6.0	17-29 25-30	B	116 & 90	Synchronization likelihood	(1) Lower characteristic path length in AD. (2) Increased synchronization in the frontal cortices and decreased synchronization in the parietal and occipital regions in AD.
Drzezga *et al.*, 2011[57]	fMRI	PiB^+ MCI PiB^+ HC PiB^- HC	13 (9) 12 (4) 12 (5)	75.9 ± 6.4 74.5 ± 5.7 71.3 ± 6.3	27.5 ± 2.43 29.42 ± 0.79 28.92 ± 0.79	B	voxel wise	Pearson's correlation	(1) Significant disruptions of whole-brain connectivity in typical cortical hubs (posterior cingulate cortex/precuneus) of amyloid-positive MCI. (2) Subtle connectivity disruptions and hypometabolism in amyloid-positive HC.
Liu *et al.*, 2012[59]	fMRI	AD MCI HC	18 (9) 16 (9) 18 (10)	43-76 54-81 49-78	17.1 ± 2.8 24.8 ± 1.4 29.5 ± 0.5	B	90	Partial correlation	(1) Highest characteristic path length and highest clustering coefficient in the AD group among the three groups. (2) Intermediate values of the small world measures in MCI networks. (3) Abnormal nodal centrality in MCI patients vs in HC and in AD *vs* in MCI.
Wang *et al.*, 2012[56]	fMRI	MCI HC	37 (17) 47 (20)	41-79 50-79	16-30 20-30	W	1024	Wavelet correlation	(1) Decreased functional connectivity and increased characteristic path length in aMCI. (2) Targeted key nodes predominantly in the default-network regions, key links primarily in the intramodular connections with the default-mode network and the intermodular connections among different functional systems in aMCI.
Zhao *et al.*, 2012[53]	fMRI	AD HC	33 (13) 20 (10)	66.2 ± 9.6 63.0 ± 5.8	15.3 ± 2.9 27.8 ± 1.3	B	90	Pearson's correlation	(1) Higher local efficiency and lower global efficiency in AD. (2) Disrupted brain regions in the default mode network, the temporal lobe and subcortical structures in AD.
Bai *et al.*, 2013[58]	fMRI	MCI HC	12 (1) 12 (4)	59.3 ± 3.3 60.6 ± 5.8	26.4 ± 0.9 29.8 ± 0.4	B	90	Partial correlation	(1) Higher characteristic path length and clustering coefficient in MCI. (2) Enhanced nodal centrality in the abnormal regions of MCI, including the hippocampus and postcentral cortex as well as the anterior cingulate cortex, with acupuncture with deep needling.
Brier *et al.*, 2013[61]	fMRI	CDR 1 CDR 0.5 CDR 0	31 (13) 90 (36) 205 (66)	70.7 ± 11.4 74.5 ± 7.5 66.4 ± 9.8	20 ± 4.5 27 ± 2.8 29 ± 1.5	B	160	Pearson's correlation	(1) Lower clustering coefficient and modularity in AD. (2) Lower clustering coefficient and modularity in cognitively normal participants with harboring AD biomarker pathology. (3) Modularity was significantly affected by age.
Chen *et al.*, 2013[54]	fMRI	AD HC	30 (17) 30 (16)	76.7 ± 5.28 75.9 ± 6.42	24.8 ± 2.97 29.4 ± 1.03	W	116	Pearson's correlation	(1) The largest homotopic module (defined as the insula module) in the HC group was broken down to the pieces in the AD group. (2) The functional connectivity changes and structural changes in the insula module have great potential as AD biomarkers.
Li *et al.*, 2013[55]	fMRI	AD HC	10 (4) 11 (4)	52-81 55-82	nr nr	B	90	Pearson's correlation	(1) Lower global efficiency and clustering coefficient in the AD group. (2) The topology parameters of the evolution network tended toward those of the AD group.
Liu *et al.*, 2013[60]	fMRI	Severe AD Mild AD MCI HC	18 (9) 17 (8) 18 (10) 21 (7)	51-82 51-75 53-81 51-84	0-15 3-25 9-28 24-30	W	442	Wavelet correlation	(1) Long distance connectivity decreased in severe AD. (2) Lower global efficiency in severe AD. (3) Altered imaging measures are correlated with MMSE.

*Range or mean ± SD. AD, Alzheimer's disease; aMCI, amnestic MCI; B, binary; CDR, clinical dementia rating; DTI, diffusion tensor imaging; EEG, electroencephalograph; eMCI, early MCI; fMRI, functional MRI; FTLD, frontotemporal lobar degeneration; HC, healthy control; lMCI, late MCI; MCI, mild cognitive impairment; MD aMCI, multidomain aMCI; MEG, magnetoencephalograph; RGD, remitted geriatric depression; MMSE, Mini Mental State Examination; nr, not reported; PiB, Pittsburgh Compound B; SD aMCI, single-domain MCI; sMRI, structural MRI; W, weighted.

Structural MRI networks In recent years, coordinated variations in brain morphology (e.g., gray-matter volume and thickness) have been used as measures of structural association between regions to construct large-scale structural correlation networks[22, 23]. This approach relies on the hypothesis that connectivity confers a mutually trophic effect on the growth of connected regions[24, 25]. In AD studies, He *et al.*[26] were the first to use cortical thickness measurement by sMRI to investigate large-scale structural networks in 92 AD patients and 97 healthy controls (HCs). They found that although both groups exhibited small-world topology in their sMRI networks, the AD patients had larger clustering coefficients and longer characteristic path lengths than controls, implying a greater segregation and a disrupted integration topological organization in AD. In addition, He and others found decreased betweenness centrality in several heteromodal association cortices (e.g., superior temporal gyrus and angular gyrus) in AD. All of these regions were identified as hubs in the healthy brain networks. The abnormalities of nodal centrality in AD also reflected a disrupted integration of brain networks. A subsequent study used three groups, AD, MCI, and HCs, to investigate the characteristics of the cortical volume network[27]. Consistently, larger clustering coefficients and longer characteristic path lengths were found in AD; and the MCI network had values intermediate between HC and AD, although no statistically significant changes were found. Further, they found loss of betweenness centrality of hub regions in the temporal lobe in the MCI and AD groups. In contrast, Tijms *et al.*[28] investigated the graph properties of a single-individual gray-matter network in AD and found decreases in clustering coefficients, characteristic path lengths, normalized clustering coefficients, and normalized characteristic path lengths.

In summary, the three sMRI-based network studies demonstrated that AD has aberrant morphological organization in sMRI networks. Specifically, two studies suggested a greater segregation and a disrupted integration of topological organization in AD based on the network construction across subjects[26, 27]. The other study implied a disrupted segregation and a more integrated topological organization in AD based on the network construction in a single individual[28]. The discrepancies in these results may be due to the differences in network construction approaches and in AD populations.

Diffusion MRI networks In addition to sMRI, the patterns of structural connectivity of the human brain *in vivo* can also be studied with dMRI tractography. dMRI maps the local diffusivity of water molecules in brain tissues[29]. Neural tractography (so-called fiber tracking) by propagating the orientation information in each voxel has proved useful for mapping white-matter trajectories[30]. By linking the distinct regions with fiber tracts, it is possible to reveal white-matter anatomical connections and to map the whole-brain connectivity. Several recent studies have used dMRI data to construct human brain white-matter networks[31-33]. In AD brain network studies, Lo *et al.*[34] for the first time used dMRI tractography to construct the networks of AD patients and HCs. In this study, the fiber number between two cortical regions multiplied by the mean fractional anisotropy of the fiber bundles was calculated as the edge weight. They found that both groups had a small-world topology and that the characteristic path length and normalized characteristic path length were increased in the AD group compared with controls, which reflected a disrupted integration of the network in AD. This result was consistent with previous sMRI brain networks in AD[26, 27]. Another similar study from Reijmer *et al.*[35] used the fiber number as the edge weight to construct white-matter networks for AD and HCs, and found a tendency toward lower clustering coefficients in AD. This result implied disruption of the information segregation ability. Recently, increasing numbers of researchers are concerned about the network characteristics of different types and different periods of MCI[36, 37]. Shu *et al.*[36] investigated the topological alterations of white-matter networks in patients with different types of amnestic MCI (aMCI). They found that the global topological properties (i.e., normalized clustering coefficients, characteristic path length, and normalized characteristic path length) of white-matter networks were significantly increased in patients with multidomain aMCI, but not in those with single-domain aMCI, compared with HCs. Meanwhile, Daianu *et al.*[37] demonstrated increased normalized clustering coefficients and decreased normalized characteristic path lengths of the white-matter network in AD, and both early and late MCI showed intermediate values with no significant difference between the HC and AD groups. Notably, Bai *et al.*[38] considered high-risk groups such as patients with remitted geriatric depression and aMCI for developing

AD. They revealed higher characteristic path lengths in the patient groups compared with HCs, and there were no significant differences in the global network properties between the patient groups. They also found that the deficits in the regional and connectivity characteristics of the patient groups were primarily in the frontal regions in the dMRI network. These results suggest that the patterns of dMRI networks in remitted geriatric depression and aMCI are very similar, which may lead to increasing attention on defining the population at risk of AD.

In summary, the five dMRI studies (2 AD, 2 MCI and 1 AD/MCI) demonstrated abnormal white-matter connectomics in both the AD and MCI groups. Of the AD studies, one suggested a disrupted integration topological organization in patients[34], and the other implied disrupted segregation[35]. Different from the two studies, Daianu *et al.*[37] implied a more segregated and a more integrated topological organization in AD compared with HCs. These discrepancies may be due to the differences in data acquisition methods and parcellation atlases: Daianu *et al.*[37] obtained dMRI data from 13 sites and parcellated the brain into 68 ROIs based on a prior FreeSurfer defined atlas, while Lo *et al.*[34] and Reijmer *et al.*[35] obtained dMRI data from single sites and parcellated the brain into 78 or 90 ROIs based on the automated anatomical labeling atlas. In addition, clinical differences in AD populations may also partly contribute to the discrepancies: in the studies by Lo *et al.*[34] and Reijmer *et al.*[35], the mean Mini-Mental State Examination (MMSE) scores of AD patients were >20, but the Daianu *et al.* study[37] did not report this measure. Of the MCI studies, two suggested the disruption of integration topological organization in MCI[36, 38], and one demonstrated more segregation in MCI[36].

Functional Connectomics in AD and MCI

The network of functional connectomics in the human brain *in vivo* can be constructed from EEG/MEG and fMRI data. In this section, we review recent progress in analyzing the functional networks in AD and MCI.

EEG/MEG networks EEG and MEG measure changes in the electric and magnetic fields related to neuronal activity at high temporal resolution (milliseconds). Several recent studies have used EEG/MEG data to construct human brain functional networks in healthy individuals[39-41]. In AD brain network studies, the first graph theoretical network analysis by Stam *et al.*[42] measured the resting-state functional connectivity of beta band-filtered EEG channels (13–30 Hz) in AD and HC groups. Although both groups showed small-world properties in their networks, the AD patients had longer characteristic path lengths. This pattern suggested a disrupted integration topological organization in AD. Later, the same research group used resting-state MEG data to investigate the functional brain network at multiple frequency bands (delta [0.5–4 Hz], theta [4–8 Hz], lower alpha [8–10 Hz], upper alpha [10–13 Hz], beta [13–30 Hz] and gamma [30–45 Hz]) in AD[43]. In the lower alpha band, the characteristic path length was increased, and the clustering coefficient, normalized clustering coefficient, and normalized characteristic path length were decreased in AD patients. In particular, AD patients had significantly lower left fronto-parietal, fronto-temporal, parieto-occipital and temporo-occipital connectional strength. These findings support a model in which AD patients exhibit disrupted segregation topological organization. In a later study, de Haan *et al.*[44] also investigated topological changes in functional brain networks in AD and frontotemporal dementia using resting-state EEG data at multiple frequency bands. In AD, the normalized clustering coefficient was decreased in the lower alpha (8–10 Hz) and beta (13–30 Hz) bands, and the normalized characteristic path length was decreased in the lower alpha and gamma bands (30–45 Hz), compared to HCs. In frontotemporal dementia, no significant differences from HCs were found in these measures. These results implied a disrupted segregation and greater integrated topological organization in AD. Next, de Haan *et al.*[45] investigated the modular structure of AD using resting-state MEG data. In AD, the delta and theta bands showed increases in modularity, while the beta and gamma bands showed strong decreases. The AD patients also showed a loss of module number in the theta, beta, and gamma bands. Decreases were found in the intra-module connections in the beta band and in the inter-module connections in the delta and theta bands. The parietal cortex showed the greatest intra-modular connections in HCs, and showed the strongest intra-modular loss in the AD group. In the same year in another study[46], de Haan and colleagues used MEG recordings in the same groups as above and used graph-spectral analysis to explore the functional networks in AD. They found lower eigenvector centrality of the left temporal region in the theta band and the parietal region in the beta

band in AD. In MCI brain network studies, Buldu *et al.*[47] evaluated the functional network of MCI using MEG data during a memory task. Five frequency bands [α_1: (8–11) Hz, α_2: (11–14) Hz, β_1: (14–25) Hz, β_2: (25–35) Hz, γ: (35–45) Hz] were considered. Graphs from MCI subjects showed an enhancement of the connection strength, suggesting that memory processing in MCI individuals is associated with higher energy expenditure. The MCI group also showed lowered normalized clustering coefficient and characteristic path length in the broadband signal.

In summary, the six EEG/MEG studies demonstrated abnormal functional brain connectomics in the AD and MCI groups, and these abnormalities are frequency dependent. These studies consistently demonstrated disrupted segregation in AD, more integrated topological organization in AD and MCI in the lower alpha band, and disrupted integration of topological organization in the beta and gamma bands in AD.

Functional MRI networks In contrast to the EEG/MEG techniques, fMRI has relatively poor temporal resolution (~2 s) but high spatial resolution (~2 mm). Resting-state fMRI measures the endogenous or spontaneous brain activity as low-frequency fluctuations in blood oxygen level-dependent (BOLD) signals[48]. Several recent studies used resting-state fMRI to construct functional networks in healthy people, and all showed small-world organization[49, 50].

For AD studies, Supekar *et al.*[51] first examined the whole-brain functional network in AD using resting-state fMRI. In the low-frequency interval of 0.01–0.05 Hz, they found significantly lower normalized clustering coefficients, especially for the bilateral hippocampus, indicative of disrupted segregated organization. Further investigation showed that using the normalized clustering coefficient as a biomarker to diagnose AD would yield up to 72% sensitivity and 78% specificity, suggesting that the topological network indices could serve as biomarkers of AD. They also found decreases in intratemporal connections and in connections between the thalamus and the frontal, temporal, and occipital lobes. In a subsequent study, Sanz-Arigita *et al.*[52] found a significantly decreased characteristic path length in the AD group. Decreased connection strengths were also found between the temporal lobe and the parietal and occipital regions. Zhao *et al.*[53] investigated the topological properties of resting-state fMRI with a focus on moderate AD, showing increases in the clustering coefficient, characteristic path length, normalized clustering coefficient, and normalized characteristic path length in the AD group. From the module perspective, Chen *et al.*[54] demonstrated that the largest homotopic module (defined as the insula module) in the HC group was divided into pieces in the AD group. They further quantified the functional connectivity changes and gray-matter concentration changes in the insula module as biomarkers for the classification of HC and AD and obtained 94% of the area under the curve of the receiver operation characteristic. These results implied a disruption of segregation topological organization in AD, and these disruptions could serve as biomarkers of AD. From a computational model perspective, Li *et al.*[55] found decreases in global efficiency (i.e., increased characteristic path lengths) and clustering coefficients in AD. They then used the node betweenness and Euclidean distance between nodes as control factors for the brain network evolution processing from one network to another. The topological properties of the evolution networks were closer to those of the AD group than of the HC group. These results suggested that network evolution could be used to study the changes in functional brain networks in AD.

In MCI studies, Wang *et al.*[56] first used resting-state fMRI and graph theory approaches to systematically investigate the topological organization of the functional connectomes in patients with aMCI and in HCs, and revealed an increased characteristic path length of connectomics in the aMCI group. Moreover, the disease targeted several key nodes, predominantly in the default-mode regions, as well as key links, primarily in the intra-module connections within the default-mode network and the inter-module connections among different functional systems. Intriguingly, the topological aberrations correlated with the patients' memory performance and could distinguish aMCI patients from HCs with a sensitivity of 86.5% and a specificity of 85.1%. Drzezga *et al.*[57] investigated the cortical hub pattern in Pittsburgh compound B (PiB)-positive MCI, PiB-positive HCs, and PiB-negative HCs using resting-state fMRI. PiB positivity indicates an increased amyloid-beta burden. These results showed significant abnormal connectivity in typical cortical hubs (posterior cingulate cortex/precuneus) in PiB-positive MCI. Importantly, subtle connectivity disruptions and hypometabolism were already present in PiB-positive

HCs. More recently, Bai *et al.*[58] explored the influence of acupuncture on the network organization of MCI from the treatment perspective. These results showed longer characteristic path lengths and larger clustering coefficients in MCI compared with HCs. In addition, acupuncture with deep needling enhanced the nodal centrality primarily in the abnormal regions of MCI, including the hippocampus, postcentral cortex, and anterior cingulate cortex, most of which present decreased node centralities in MCI.

Three other resting-state fMRI studies compared the brain network attributes of AD, MCI, and HC groups[59-61]. Liu *et al.*[59] found that AD patients had the longest characteristic path lengths and the largest clustering coefficients, while the small-world measures of MCI networks exhibited intermediate values but showed no significant changes compared with HCs. In addition, another study conducted by Liu *et al.*[60] found decreased global efficiency (i.e., increased characteristic path lengths) and loss of long-distance connectivities in the AD group, implying disrupted integration topological organization. Recently, Brier *et al.*[61] investigated graph theory metrics as a function of disease severity. Decreased clustering coefficient and modularity were observed with increasing Clinical Dementia Rating, and these decreases also appeared in normal participants who harbored AD biomarker pathology.

In summary, the eleven resting-state fMRI studies (5 AD, 3 MCI, and 3 AD/MCI studies) demonstrated abnormal functional brain connectomics in the AD and MCI groups. In AD research, four studies suggested a disrupted integration topological organization in AD[53, 55, 59, 60], whereas one suggested an enhanced integration topological organization[52]. The discrepancies in these results may be due to differences in network construction approaches. Sanz-Arigita *et al.*[52] used a synchronization likelihood method to calculate the functional connectivity, while other studies used time-series correlations (partial correlation or Pearson's correlation) to calculate the connectivity. In addition, two studies implied greater segregation[53, 59] but four implied disrupted segregation topological organization in AD[51, 54, 55, 61]. The discrepancies in these results may be due to differences in the AD populations. The two studies showing patterns of greater segregation recruited AD patients with mean MMSE scores <18, and the four studies showing disrupted segregation organization recruited AD patients with mean MMSE scores >18. Patients at different stages may manifest different behavioral symptoms with distinct underlying neuronal mechanisms. In MCI research, three studies demonstrated a disrupted integration topological organization[56-58], and one suggested more segregation[58] in MCI.

Different Changing Patterns between Connectome-based AD/MCI Studies

Overall, the studies of structural and functional brain connectomics in AD and MCI have demonstrated that the network configuration in patients is significantly different from HCs. However, it must be noted that the changes of topological configuration in the networks exhibited distinct patterns in different modalities and populations (i.e., AD and MCI) (Fig. 2). These discrepancies may be caused by different imaging techniques providing different views of brain structure and function: structural MRI provides information about the morphology of gray matter; dMRI provides information about structural connectivity among brain regions; EEG/MEG measures the changes in the electrical and magnetic fields associated with neuronal activity at high temporal resolution (milliseconds); and resting-state fMRI measures the endogenous or spontaneous brain activity as low-frequency fluctuations in BOLD signals. In addition, these studies recruited different AD populations, involving different preclinical and clinical stages. Recently, Brier *et al.*[61] demonstrated that the changes in network topological metrics are related to clinical AD status. Thus, all of these factors may have affected the consistency of the network analysis results. Nonetheless, these studies commonly point to a less-optimized connectivity pattern in the brain networks of AD and MCI patients.

Methodological Issues and Future Perspectives

In this review, we summarized the recent findings of disrupted structural and functional brain connectivity in AD and MCI using sMRI, dMRI, EEG/MEG, and resting-state fMRI data. Most of these studies demonstrated that AD and MCI brain networks have a disrupted segregated and integrated topological organization. Network analysis methods have enabled relatively comprehensive mapping of brain connectivity and topological organization. In particular, the application of network analysis to AD has led to novel insights into how this disease affects distributed

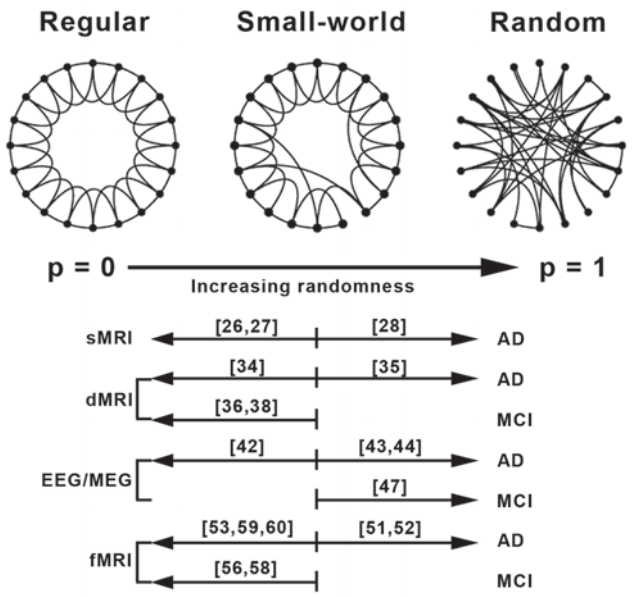

Fig. 2. Schematic of small-world networks and overview of main model findings of large-scale structural and functional brain network studies in AD and MCI. The computational model of small-world networks proposed by Watts and Strogatz (1998) begins by connecting nodes with their nearest neighbors, producing a regular network that has a high clustering coefficient and long characteristic path length. With a probability *P*, edges are then randomly rewired. When *P* is equal to unity, all edges are randomly rewired, and thus the network is perfectly random, with a low clustering coefficient and short characteristic path length. However, when *P* is between 0 and 1, the graph is a small-world network: a shorter characteristic path length, like a random network, and a greater clustering coefficient, like a regular network. Based on the small-world models, the brain network studies in AD and MCI can be classified as favoring a more regular (left arrow) and random (right arrow) configuration. Numbers in brackets indicate corresponding reference number.

neuronal circuits. However, network-based analysis is a double-edged sword because it primarily addresses the interactions among elements (e.g., voxels and regions) and ignores the focal information of individual elements. Imaging data can also carry local features of brain structure and function such as the regional morphology (gray matter volume and thickness) obtained from sMRI data and local activation information from EEG/MEG/fMRI. Combination of these regional and connectivity features is important for deepening our understanding of brain function. In addition, researchers should be aware that the studies of complex brain networks in AD and MCI are in their early stages. There are still a number of challenging issues and further considerations remaining for understanding the changed topological organization of brain networks in AD and MCI.

First, given that the human connectome represents the complete set of neuronal elements and inter-element connections composing the brain[62], appropriately defining the nodes and edges in a brain network is required. Due to the vast numbers of neurons and interconnections, reconstructing an entire brain connectome on the neuronal level is an ambitious and challenging task that requires advances in both imaging techniques and computer systems. Currently, the connectomics of the human brain is instead formed on the regional or voxel level. However, there is no gold standard for the construction of brain networks. Various parcellation schemes, such as anatomical templates, random templates, functional templates, and voxel-based schemes, can be used to define the nodes for such networks. Recent findings have demonstrated the important influences of node choices on the properties of the resulting networks[63, 64]. Therefore, researchers should be cautious when collating results of studies that use different parcellation schemes. In AD brain connectome studies, the numbers of nodes range from ~24 to 8683. This may lead to inconsistent results. However, it is also important to identify the parcellation scheme that is most sensitive for detection of AD.

Second, in parallel with the definition of nodes, the method for defining the edges in brain networks is also important. Various definition choices are currently available for estimating the connectivity, such as gray-matter morphological correlation in sMRI, fiber number, fiber length, fractional anisotropy for dMRI, and Pearson's correlation, partial correlation, or wavelet correlation for fMRI. Different definitions focus on different brain attributes (fiber number, fiber length) or different synchrony relations (linear or nonlinear). One recent study has demonstrated significant connectivity-related differences in the topological organization of resting-state networks[65]. In addition, there are three common threshold rules used to construct binary or weighted brain networks. The equi-sparse threshold rule uses different thresholds for each individual to ensure that all networks in the group have the same number of edges or sparsity. The equi-thresholds method uses the same threshold for each individual, meaning that the networks

usually have different numbers of edges. In the statistically significant correlation method, the statistically significant correlation edges are maintained in the network. Different threshold rules may lead to different network topological organizations. Importantly, using the equi-thresholds and statistically significant correlation rules, the results of network properties compared between groups may differ from the results of normalized network properties because there are different degrees of distribution of matched random networks in different individuals. In particular, the increased characteristic path lengths in AD compared with HC may accompany the decreased normalized characteristic path lengths in AD because the characteristic path length distribution obtained from the random network of an individual is different from that of other people using these rules. In fact, such seemingly contradictory results were indeed found in an AD study[43].

Third, while graph theoretical approaches provide valuable insights into normal brain architecture and the pathological mechanisms of neurological and psychiatric diseases, the test-retest reliability of graphic metrics is important for reaching convincing conclusions. These metrics may be affected by many factors, involving acquisition parameters[66-68], fluctuations of conscious states[69-71], selection of preprocessing strategies[72, 73], and network construction approaches (e.g., different nodal and edge definitions)[68, 74, 75]. Therefore, choosing reliable analytical schemes and network metrics of interest is very important for brain network studies in both healthy and diseased populations.

Fourth, there are two major types of AD, early-onset and the more common late-onset. The presence of the apolipoprotein E (APOE) gene with allelic variant 4 (*APOE* ε4) is the most important genetic risk factor for late-onset AD, together with age[76]. Brown *et al.*[77] recently demonstrated that *APOE* ε4 carriers have an accelerated age-related loss of the clustering coefficients using diffusion tensor imaging, especially for the precuneus and cingulate regions. More recently, Zhao *et al.*[53] found that the *APOE* ε4 genotype modulated the topological properties of brain functional networks derived from resting-state fMRI in the AD group. They showed a decreasing tendency of clustering coefficients and characteristic path lengths in AD *APOE* ε4 carriers compared with non-carriers. Thus, the differences in topological parameters between the two AD groups may reflect different neurological functional impairments. However, how *APOE* ε4 and other genetic risk factors of AD affect the topology of the human connectome in healthy aging and AD, and the underlying mechanisms of these differences, remain to be further systematically explored.

Fifth, the core neuropathologies in AD include abnormalities such as the accumulation of the protein amyloid-beta (Aβ) and the development of neurofibrillary tangles[78, 79]. Such changes occur decades before the onset of AD. The detection of Aβ in the brains of living subjects has been made possible by the introduction of molecular imaging techniques such as positron emission tomography with Pittsburgh compound B. Buckner *et al.*[80] demonstrated high Aβ deposition in AD compared with elderly controls in locations corresponding with the hub regions of young, healthy brain networks, within the posterior cingulate, lateral temporal, lateral parietal, and medial/lateral prefrontal cortices. Further, Drzezga *et al.*[57] found that whole-brain connectivity values showed a negative correlation with Aβ deposition in the posterior cingulate cortex across their entire sample, including MCI and HCs. However, the relationship between these pathological changes (e.g., Aβ deposition) and network abnormalities requires further exploration. Empirical studies of AD pathology and neuroimaging would be helpful for clarifying this issue.

Sixth, the use of computational simulation models is important for understanding disease progression. Recently, de Hann *et al.*[81] used a computational model to test the hypothesis that hub regions are preferentially affected due to high neuronal activity levels in AD. They demonstrated the 'activity-dependent degeneration' hypothesis of AD. Two study groups used graph theory to suggest that neurodegenerative diseases spread diffusively *via* intrinsic brain networks[82, 83]. Li *et al.*[55] used the node betweenness and Euclidean distance between nodes as the control factors of the brain network evolution processing from one network to another and found that the topological properties of evolution networks were more like those of the AD group than those of the HC group. Further work is still needed to deepen our understanding of AD pathology, including the source spatial positions of AD and the disease diffusion patterns.

Finally, preclinical AD has been proposed as one of the

three stages of AD. However, no gold-standard diagnostic criteria have been provided. The generation of imaging biomarkers for this stage is urgent. In other words, it is vital to explore the initiation phase of AD. Further, longitudinal and multimodal imaging studies would be helpful for a comprehensive understanding of the pathophysiological sequence of events and would provide valuable insights into the cognitive deficits in AD.

Conclusions

Taken together, the converging findings from these multi-modal neuroimaging and neurophysiological studies suggest that AD is associated with disrupted integration and segregation in large-scale brain networks and that these disruptions may be responsible for the cognitive deficits. Thus, these connectome-based studies provide further support for the notion of AD as a disconnection syndrome and open a new window into our understanding of the pathophysiological mechanisms of this disease. These studies also have important implications for uncovering imaging biomarkers for clinical diagnosis and treatment evaluation of AD.

ACKNOWLEDGEMENTS

This review was supported by National Key Basic Research Program of China (2014CB846102), Natural Science Foundation of China (81030028 and 31221003), Beijing Natural Science Foundation (Z111107067311036) and National Science Fund for Distinguished Young Scholars (81225012).

Received date: 2013-12-11; Accepted date: 2014-01-23

REFERENCES

[1] Albert MS, DeKosky ST, Dickson D, Dubois B, Feldman HH, Fox NC*, et al.* The diagnosis of mild cognitive impairment due to Alzheimer's disease: Recommendations from the National Institute on Aging-Alzheimer's Association workgroups on diagnostic guidelines for Alzheimer's disease. Alzheimers Dement 2011, 7: 270–279.

[2] Jack Jr CR, Albert MS, Knopman DS, McKhann GM, Sperling RA, Carrillo MC*, et al.* Introduction to the recommendations from the National Institute on Aging-Alzheimer's Association workgroups on diagnostic guidelines for Alzheimer's disease. Alzheimers Dement 2011, 7: 257–262.

[3] McKhann GM, Knopman DS, Chertkow H, Hyman BT, Jack Jr CR, Kawas CH*, et al.* The diagnosis of dementia due to Alzheimer's disease: Recommendations from the National Institute on Aging-Alzheimer's Association workgroups on diagnostic guidelines for Alzheimer's disease. Alzheimers Dement 2011, 7: 263–269.

[4] Sperling RA, Aisen PS, Beckett LA, Bennett DA, Craft S, Fagan AM*, et al.* Toward defining the preclinical stages of Alzheimer's disease: Recommendations from the National Institute on Aging-Alzheimer's Association workgroups on diagnostic guidelines for Alzheimer's disease. Alzheimers Dement 2011, 7: 280–292.

[5] Petersen RC, Smith GE, Waring SC, Ivnik RJ, Tangalos EG, Kokmen E. Mild cognitive impairment: clinical characterization and outcome. Arch Neurol 1999, 56: 303–308.

[6] Delbeuck X, Van der Linden M, Collette F. Alzheimer's disease as a disconnection syndrome? Neuropsychol Rev 2003, 13: 79–92.

[7] Delbeuck X, Collette F, Van der Linden M. Is Alzheimer's disease a disconnection syndrome? Neuropsychologia 2007, 45: 3315–3323.

[8] Bozzali M, Parker GJM, Serra L, Embleton K, Gili T, Perri R*, et al.* Anatomical connectivity mapping: A new tool to assess brain disconnection in Alzheimer's disease. Neuroimage 2011, 54: 2045–2051.

[9] Bullmore E, Sporns O. Complex brain networks: graph theoretical analysis of structural and functional systems. Nat Rev Neurosci 2009, 10: 186–198.

[10] Bullmore E, Sporns O. The economy of brain network organization. Nat Rev Neurosci 2012, 13: 336–349.

[11] Kelly C, Biswal BB, Craddock RC, Castellanos FX, Milham MP. Characterizing variation in the functional connectome: promise and pitfalls. Trends Cogn Sci 2012, 16: 181–188.

[12] Boccaletti S, Latora V, Moreno Y, Chavez M, Hwang D. Complex networks: Structure and dynamics. Physics Rep 2006, 424: 175–308.

[13] Rubinov M, Sporns O. Complex network measures of brain connectivity: uses and interpretations. Neuroimage 2010, 52: 1059–1069.

[14] Sporns O. Network attributes for segregation and integration in the human brain. Curr Opin Neurobiol 2013, 23: 162–171.

[15] Newman ME. Modularity and community structure in networks. Proc Natl Acad Sci U S A 2006, 103: 8577–8582.

[16] Freeman LC. Centrality in social networks conceptual clarification. Soc Networks 1979, 1: 215–239.

[17] Bonacich P. Factoring and weighting approaches to status scores and clique identification. J Math Sociol 1972, 2: 113–120.

[18] Watts DJ, Strogatz SH. Collective dynamics of 'small-world' networks. Nature 1998, 393: 440–442.

[19] He Y, Chen Z, Gong G, Evans A. Neuronal networks in

Alzheimer's disease. Neuroscientist 2009, 15: 333–350.
[20] Xie T, He Y. Mapping the Alzheimer's brain with connectomics. Front Psychiatry 2011, 2: 77.
[21] Tijms BM, Wink AM, de Haan W, van der Flier WM, Stam CJ, Scheltens P*, et al.* Alzheimer's disease: connecting findings from graph theoretical studies of brain networks. Neurobiol Aging 2013, 34: 2023–2036.
[22] He Y, Chen ZJ, Evans AC. Small-world anatomical networks in the human brain revealed by cortical thickness from MRI. Cereb Cortex 2007, 17: 2407–2419.
[23] Bassett DS, Bullmore E, Verchinski BA, Mattay VS, Weinberger DR, Meyer-Lindenberg A. Hierarchical organization of human cortical networks in health and schizophrenia. J Neurosci 2008, 28: 9239–9248.
[24] Wright IC, Sharma T, Ellison ZR, McGuire PK, Friston KJ, Brammer MJ*, et al.* Supra-regional Brain Systems and the Neuropathology of Schizophrenia. Cereb Cortex 1999, 9: 366–378.
[25] Pezawas L, Meyer-Lindenberg A, Drabant EM, Verchinski BA, Munoz KE, Kolachana BS*, et al.* 5-HTTLPR polymorphism impacts human cingulate-amygdala interactions: a genetic susceptibility mechanism for depression. Nat Neurosci 2005, 8: 828–834.
[26] He Y, Chen Z, Evans A. Structural insights into aberrant topological patterns of large-scale cortical networks in Alzheimer's disease. J Neurosci 2008, 28: 4756–4766.
[27] Yao Z, Zhang Y, Lin L, Zhou Y, Xu C, Jiang T. Abnormal cortical networks in mild cognitive impairment and Alzheimer's disease. PLoS Comput Biol 2010, 6: e1001006.
[28] Tijms BM, Moller C, Vrenken H, Wink AM, de Haan W, van der Flier WM*, et al.* Single-subject grey matter graphs in Alzheimer's disease. PLoS One 2013, 8: e58921.
[29] Le Bihan D. Looking into the functional architecture of the brain with diffusion MRI. Nat Rev Neurosci 2003, 4: 469–480.
[30] Mori S, van Zijl PC. Fiber tracking: principles and strategies - a technical review. NMR Biomed 2002, 15: 468–480.
[31] Hagmann P, Kurant M, Gigandet X, Thiran P, Wedeen VJ, Meuli R*, et al.* Mapping human whole-brain structural networks with diffusion MRI. PLoS One 2007, 2: e597.
[32] Gong G, He Y, Concha L, Lebel C, Gross DW, Evans AC*, et al.* Mapping anatomical connectivity patterns of human cerebral cortex using in vivo diffusion tensor imaging tractography. Cereb Cortex 2009, 19: 524–536.
[33] Iturria-Medina Y, Sotero RC, Canales-Rodriguez EJ, Aleman-Gomez Y, Melie-Garcia L. Studying the human brain anatomical network via diffusion-weighted MRI and Graph Theory. Neuroimage 2008, 40: 1064–1076.
[34] Lo CY, Wang PN, Chou KH, Wang J, He Y, Lin CP. Diffusion tensor tractography reveals abnormal topological organization in structural cortical networks in Alzheimer's disease. J Neurosci 2010, 30: 16876–16885.
[35] Reijmer YD, Leemans A, Caeyenberghs K, Heringa SM, Koek HL, Biessels GJ. Disruption of cerebral networks and cognitive impairment in Alzheimer disease. Neurology 2013, 80: 1370–1377.
[36] Shu N, Liang Y, Li H, Zhang J, Li X, Wang L*, et al.* Disrupted topological organization in white matter structural networks in amnestic mild cognitive impairment: relationship to subtype. Radiology 2012, 265: 518–527.
[37] Daianu M, Jahanshad N, Nir TM, Toga AW, Jack CR, Jr., Weiner MW*, et al.* Breakdown of brain connectivity between normal aging and Alzheimer's disease: a structural k-core network analysis. Brain Connect 2013, 3: 407–422.
[38] Bai F, Shu N, Yuan Y, Shi Y, Yu H, Wu D*, et al.* Topologically Convergent and Divergent Structural Connectivity Patterns between Patients with Remitted Geriatric Depression and Amnestic Mild Cognitive Impairment. J Neurosci 2012, 32: 4307–4318.
[39] Stam CJ. Functional connectivity patterns of human magnetoencephalographic recordings: a 'small-world' network? Neurosci Lett 2004, 355: 25–28.
[40] Bassett DS, Meyer-Lindenberg A, Achard S, Duke T, Bullmore E. Adaptive reconfiguration of fractal small-world human brain functional networks. Proc Natl Acad Sci U S A 2006, 103: 19518–19523.
[41] Smit DJ, Boersma M, Schnack HG, Micheloyannis S, Boomsma DI, Hulshoff Pol HE*, et al.* The brain matures with stronger functional connectivity and decreased randomness of its network. PLoS One 2012, 7: e36896.
[42] Stam CJ, Jones BF, Nolte G, Breakspear M, Scheltens P. Small-world networks and functional connectivity in Alzheimer's disease. Cereb Cortex 2007, 17: 92–99.
[43] Stam CJ, de Haan W, Daffertshofer A, Jones BF, Manshanden I, van Cappellen van Walsum AM*, et al.* Graph theoretical analysis of magnetoencephalographic functional connectivity in Alzheimer's disease. Brain 2009, 132: 213–224.
[44] de Haan W, Pijnenburg YA, Strijers RL, van der Made Y, van der Flier WM, Scheltens P*, et al.* Functional neural network analysis in frontotemporal dementia and Alzheimer's disease using EEG and graph theory. BMC Neurosci 2009, 10: 101.
[45] de Haan W, van der Flier WM, Koene T, Smits LL, Scheltens P, Stam CJ. Disrupted modular brain dynamics reflect cognitive dysfunction in Alzheimer's disease. Neuroimage 2012, 59: 3085–3093.
[46] de Haan W, van der Flier WM, Wang H, Van Mieghem PF, Scheltens P, Stam C. Disruption of functional brain networks in Alzheimer's disease: what can we learn from graph spectral analysis of resting-state MEG? Brain Connect 2012, 2: 45–55.

[47] Buldu JM, Bajo R, Maestu F, Castellanos N, Leyva I, Gil P, *et al.* Reorganization of functional networks in mild cognitive impairment. PLoS One 2011, 6: e19584.

[48] Biswal B, Yetkin FZ, Haughton VM, Hyde JS. Functional connectivity in the motor cortex of resting human brain using echo-planar MRI. Magn Reson Med 1995, 34: 537–541.

[49] Salvador R, Suckling J, Coleman MR, Pickard JD, Menon D, Bullmore E. Neurophysiological architecture of functional magnetic resonance images of human brain. Cereb Cortex 2005, 15: 1332–1342.

[50] Achard S, Salvador R, Whitcher B, Suckling J, Bullmore E. A resilient, low-frequency, small-world human brain functional network with highly connected association cortical hubs. J Neurosci 2006, 26: 63–72.

[51] Supekar K, Menon V, Rubin D, Musen M, Greicius MD. Network analysis of intrinsic functional brain connectivity in Alzheimer's disease. PLoS Comput Biol 2008, 4: e1000100.

[52] Sanz-Arigita EJ, Schoonheim MM, Damoiseaux JS, Rombouts SA, Maris E, Barkhof F, *et al.* Loss of 'small-world' networks in Alzheimer's disease: graph analysis of FMRI resting-state functional connectivity. PLoS One 2010, 5: e13788.

[53] Zhao X, Liu Y, Wang X, Liu B, Xi Q, Guo Q, *et al.* Disrupted Small-World Brain Networks in Moderate Alzheimer's Disease: A Resting-State fMRI Study. PLoS One 2012, 7: e33540.

[54] Chen G, Zhang HY, Xie C, Zhang ZJ, Teng GJ, Li SJ. Modular reorganization of brain resting state networks and its independent validation in Alzheimer's disease patients. Front Hum Neurosci 2013, 7: 456.

[55] Li Y, Qin Y, Chen X, Li W. Exploring the functional brain network of Alzheimer's disease: based on the computational experiment. PLoS One 2013, 8: e73186.

[56] Wang J, Zuo X, Dai Z, Xia M, Zhao Z, Zhao X, *et al.* Disrupted Functional Brain Connectome in Individuals at Risk for Alzheimer's Disease. Biol Psychiatry 2012, 73: 472–481.

[57] Drzezga A, Becker JA, Van Dijk KR, Sreenivasan A, Talukdar T, Sullivan C, *et al.* Neuronal dysfunction and disconnection of cortical hubs in non-demented subjects with elevated amyloid burden. Brain 2011, 134: 1635–1646.

[58] Bai L, Zhang M, Chen S, Ai L, Xu M, Wang D, *et al.* Characterizing acupuncture de qi in mild cognitive impairment: relations with small-world efficiency of functional brain networks. Evid Based Complement Alternat Med 2013, 2013: 1–7.

[59] Liu Z, Zhang Y, Yan H, Bai L, Dai R, Wei W, *et al.* Altered topological patterns of brain networks in mild cognitive impairment and Alzheimer's disease: A resting-state fMRI study. Psychiatry Res 2012, 202: 118–125.

[60] Liu Y, Yu C, Zhang X, Liu J, Duan Y, Alexander-Bloch AF, *et al.* Impaired long distance functional connectivity and weighted network architecture in Alzheimer's disease. Cereb Cortex 2013. doi: 10.1093/cercor/bhs410

[61] Brier M, Thomas J, Fagan A, Hassenstab J, Holtzman D, Benzinger T, *et al.* Functional connectivity and graph theory in preclinical Alzheimer's disease. Neurobiol Aging 2013, [Epub ahead of print].

[62] Sporns O, Tononi G, Kotter R. The human connectome: A structural description of the human brain. PLoS Comput Biol 2005, 1: e42.

[63] Wang J, Wang L, Zang Y, Yang H, Tang H, Gong Q, *et al.* Parcellation-dependent small-world brain functional networks: a resting-state fMRI study. Hum Brain Mapp 2009, 30: 1511–1523.

[64] de Reus MA, van den Heuvel MP. The parcellation-based connectome: limitations and extensions. Neuroimage 2013, 80: 397–404.

[65] Liang X, Wang J, Yan C, Shu N, Xu K, Gong G, *et al.* Effects of different correlation metrics and preprocessing factors on small-world brain functional networks: a resting-state functional MRI study. PLoS One 2012, 7: e32766.

[66] Van Dijk KR, Hedden T, Venkataraman A, Evans KC, Lazar SW, Buckner RL. Intrinsic functional connectivity as a tool for human connectomics: theory, properties, and optimization. J Neurophysiol 2010, 103: 297–321.

[67] Whitlow CT, Casanova R, Maldjian JA. Effect of resting-state functional MR imaging duration on stability of graph theory metrics of brain network connectivity. Radiology 2011, 259: 516–524.

[68] Bassett DS, Brown JA, Deshpande V, Carlson JM, Grafton ST. Conserved and variable architecture of human white matter connectivity. Neuroimage 2011, 54: 1262–1279.

[69] Greicius MD, Kiviniemi V, Tervonen O, Vainionpaa V, Alahuhta S, Reiss AL, *et al.* Persistent default-mode network connectivity during light sedation. Hum Brain Mapp 2008, 29: 839–847.

[70] Cao H, Plichta MM, Schafer A, Haddad L, Grimm O, Schneider M, *et al.* Test-retest reliability of fMRI-based graph theoretical properties during working memory, emotion processing, and resting state. Neuroimage 2014, 84: 888–900.

[71] Weber MJ, Detre JA, Thompson-Schill SL, Avants BB. Reproducibility of functional network metrics and network structure: a comparison of task-related BOLD, resting ASL with BOLD contrast, and resting cerebral blood flow. Cogn Affect Behav Neurosci 2013, 13: 627–640.

[72] Buchanan CR, Pernet CR, Gorgolewski KJ, Storkey AJ, Bastin ME. Test-retest reliability of structural brain networks from diffusion MRI. Neuroimage 2014, 86: 231–243.

[73] Liao XH, Xia MR, Xu T, Dai ZJ, Cao XY, Niu HJ, *et al.*

Functional brain hubs and their test-retest reliability: a multiband resting-state functional MRI study. Neuroimage 2013, 83: 969–982.

[74] Wang JH, Zuo XN, Gohel S, Milham MP, Biswal BB, He Y. Graph theoretical analysis of functional brain networks: test-retest evaluation on short- and long-term resting-state functional MRI data. PLoS One 2011, 6: e21976.

[75] Cheng H, Wang Y, Sheng J, Kronenberger WG, Mathews VP, Hummer TA*, et al.* Characteristics and variability of structural networks derived from diffusion tensor imaging. Neuroimage 2012, 64: 1153–1164.

[76] Leoni V. The effect of apolipoprotein E (ApoE) genotype on biomarkers of amyloidogenesis, tau pathology and neurodegeneration in Alzheimer's disease. Clin Chem Lab Med 2011, 49: 375–383.

[77] Brown JA, Terashima KH, Burggren AC, Ercoli LM, Miller KJ, Small GW*, et al.* Brain network local interconnectivity loss in aging APOE-4 allele carriers. Proc Natl Acad Sci U S A 2011, 108: 20760–20765.

[78] Hardy J, Selkoe DJ. The amyloid hypothesis of Alzheimer's disease: progress and problems on the road to therapeutics. Science 2002, 297: 353–356.

[79] Selkoe DJ. Biochemistry and molecular biology of amyloid beta-protein and the mechanism of Alzheimer's disease. Handb Clin Neurol 2008, 89: 245–260.

[80] Buckner RL, Sepulcre J, Talukdar T, Krienen FM, Liu H, Hedden T*, et al.* Cortical hubs revealed by intrinsic functional connectivity: mapping, assessment of stability, and relation to Alzheimer's disease. J Neurosci 2009, 29: 1860–1873.

[81] de Haan W, Mott K, van Straaten EC, Scheltens P, Stam CJ. Activity dependent degeneration explains hub vulnerability in Alzheimer's disease. PLoS Comput Biol 2012, 8: e1002582.

[82] Raj A, Kuceyeski A, Weiner M. A network diffusion model of disease progression in dementia. Neuron 2012, 73: 1204–1215.

[83] Zhou J, Gennatas ED, Kramer JH, Miller BL, Seeley WW. Predicting regional neurodegeneration from the healthy brain functional connectome. Neuron 2012, 73: 1216–1227.